Mineralium Deposita (2006) 40: 726–741
DOI 10.1007/s00126-005-0029-3

ARTICLE

Guoxiang Chi · Benoît Dubé · Kenneth Williamson
Anthony E. Williams-Jones

# Formation of the Campbell-Red Lake gold deposit by $H_2O$-poor, $CO_2$-dominated fluids

Received: 22 February 2005 / Accepted: 7 October 2005 / Published online: 17 November 2005


**Abstract** The Campbell-Red Lake gold deposit in the Red Lake greenstone belt, with a total of approximately 840 t of gold (past production + reserves) and an average grade of 21 g/t Au, is one of the largest and richest Archean gold deposits in Canada. Gold mineralization is mainly associated with silicification and arsenopyrite that replace carbonate veins, breccias and wallrock selvages. The carbonate veins and breccias, which are composed of ankerite ± quartz and characterized by crustiform–cockade textures, were formed before and/or in the early stage of penetrative ductile deformation, whereas silicification, arsenopyrite replacement and gold mineralization were coeval with deformation. Microthermometry and laser Raman spectroscopy indicate that fluid inclusions in ankerite and associated quartz (Q1) and main ore-stage quartz (Q2) are predominantly carbonic, composed mainly of $CO_2$, with minor $CH_4$ and $N_2$. Aqueous and aqueous–carbonic inclusions are extremely rare in both ankerite and quartz. $H_2O$ was not detected by laser Raman spectroscopic analyses of individual carbonic inclusions and by gas chromatographic analyses of bulk samples of ankerite and main ore-stage quartz (Q2). Fluid inclusions in post-mineralization quartz (Q3) are also mainly carbonic, but proportions of aqueous and aqueous–carbonic inclusions are present. Trace amounts of $H_2S$ were detected by laser Raman spectroscopy in some carbonic inclusions in Q2 and Q3, and by gas chromatographic analyses of bulk samples of ankerite and Q2. $^3He/^4He$ ratios of bulk fluid inclusions range from 0.008 to 0.016 Ra in samples of arsenopyrite and gold. Homogenization temperatures ($T_h$–$CO_2$) of carbonic inclusions are highly variable (from −4.1 to +30.4°C; mostly to liquid, some to vapor), but the spreads within individual fluid inclusion assemblages (FIAs) are relatively small (within 0.5 to 10.3°C). Carbonic inclusions occur both in FIAs with narrow $T_h$–$CO_2$ ranges and in those with relatively large $T_h$–$CO_2$ variations. The predominance of carbonic fluid inclusions has been previously reported in a few other gold deposits, and its significance for gold metallogeny has been debated. Some authors have proposed that formation of the carbonic fluid inclusions and their predominance is due to post-trapping leakage of water from aqueous–carbonic inclusions ($H_2O$ leakage model), whereas others have proposed that they reflect preferential trapping of the $CO_2$-dominated vapor in an immiscible aqueous–carbonic mixture (fluid unmixing model), or represent an unusually $H_2O$-poor, $CO_2$-dominated fluid (single carbonic fluid model). Based on the FIA analysis reported in this study, we argue that although post-trapping modifications and host mineral deformation may have altered the fluid inclusions in varying degrees, these processes were not solely responsible for the formation of the carbonic inclusions. The single carbonic fluid model best explains the extreme rarity of aqueous inclusions but lacks the support of experimental data that might indicate the viability of significant transport of silica and gold in a carbonic fluid. In contrast, the weakness of the unmixing model is that it lacks unequivocal petrographic evidence of phase separation. If the unmixing model were to be applied, the fluid prior

Editorial handling: G. Beaudoin

Geological Survey of Canada contribution 2004383.

G. Chi (✉)
Department of Geology, University of Regina,
Regina, SK, S4S 0A2, Canada
E-mail: guoxiang.chi@uregina.ca

B. Dubé
Geological Survey of Canada, Quebec,
QC, G1K 9A9, Canada

K. Williamson
INRS-ETE, Quebec, QC, G1K 9A9, Canada

K. Williamson
Goldcorp Inc., Red Lake mine, Balmertown, ON,
P0V 1C0, Canada

A. E. Williams-Jones
Department of Earth and Planetary Sciences,
McGill University, Montreal, QC, H3A 2A7, Canada

to unmixing would have to be much more enriched in carbonic species and poorer in water than in most orogenic gold deposits in order to explain the predominance of carbonic inclusions. The $H_2O$-poor, $CO_2$-dominated fluid may have been the product of high-grade metamorphism or early degassing of magmatic intrusions, or could have resulted from the accumulation of vapor produced by phase separation external to the site of mineralization.

**Keywords** Campbell-Red Lake · Gold deposits · Fluid inclusions · Carbonic · Gold transport

## Introduction

Carbon dioxide is a common component of ore-forming fluids in orogenic-type and granitic intrusion-related gold deposits (Ridley and Diamond 2000; Baker 2002; Groves et al. 2003). As summarized by Ridley and Diamond (2000), fluids responsible for the formation of porphyry- and epithermal-type gold deposits are characterized by compositions in the $H_2O$-NaCl system, with the porphyry-type having higher salinity than the epithermal types, whereas fluids forming orogenic gold deposits have compositions in the $H_2O$–$CO_2$–NaCl system, with generally low salinities. The most frequently recorded $CO_2$ mole fraction for fluid inclusions in orogenic gold deposits ranges from ~0.10 to ~0.25, and the salinities range from ~1.6 to ~5.9 wt% (based on Fig. 2 of Ridley and Diamond 2000). In addition to $CO_2$, variable proportions of $CH_4$ and $N_2$ are commonly present in the fluid inclusions and are generally grouped with $CO_2$ under the umbrella term "carbonic" (e.g., Ridley and Diamond 2000; Van den Kerkhof and Thiéry 2001).

Fluid inclusions in orogenic-type gold deposits can be divided into three categories, i.e., aqueous, aqueous–carbonic, and carbonic (Ridley and Diamond 2000). The carbonic inclusions are those in which $H_2O$ cannot be detected by visual inspection, microthermometry or laser Raman spectroscopy, whereas aqueous inclusions do not contain a visible carbonic phase. Carbonic inclusions are not called "carbonic-rich" in this paper because this term may be confused with carbonic–aqueous inclusions in which the carbonic phase is dominant and $H_2O$ is still visible (e.g., 80% $CO_2$ + 20% $H_2O$). While carbonic fluid inclusions are frequently found in orogenic gold deposits, they are generally accompanied by aqueous–carbonic inclusions, with or without aqueous inclusions (Ridley and Diamond 2000). In a few cases, however, the carbonic inclusions are almost the only type of inclusions found in the deposit, e.g., gold deposits in the Ashanti Belt, Ghana (Schmidt Mumm et al. 1997), the Bin Yauri gold deposit in Nigeria (Garba and Akande 1992), and the Fazenda Maria Preta gold deposit in Brazil (Xavier and Foster 1999). Although carbonic inclusions may be produced by fluid phase separation (e.g., Robert and Kelly 1987) and/or preferential leakage of $H_2O$ relative to the carbonic phase after entrapment (Hollister 1988, 1990; Bakker and Jansen 1994; Johnson and Hollister 1995), these mechanisms cannot satisfactorily explain why so few aqueous inclusions were entrapped and/or preserved in the above mentioned cases. Schmidt Mumm et al. (1997, 1998) proposed that the predominance of carbonic fluid inclusions in the Ashanti Belt probably indicates a new type of gold mineralizing fluid that is $H_2O$-poor, whereas Klemd (1998) argued that the phenomenon resulted from preferential leakage of $H_2O$ from aqueous–carbonic inclusions during deformation and recrystallization.

In this paper, we investigate the cause for the predominance of carbonic inclusions through detailed fluid inclusion petrography and microthermometry of the Campbell-Red Lake gold deposit in Ontario, Canada. The abundance of carbonic inclusions and rarity of aqueous inclusions in this large gold deposit have been noted in previous studies (Tarnocai 2000; Chi et al. 2002, 2003), but the origin and significance of the carbonic inclusions have not been fully discussed. The fluid inclusion assemblage (FIA) analysis method (Goldstein and Reynolds 1994) was used to evaluate whether or not a group of fluid inclusions has been subject to significant modification after entrapment—a topic of central interest when discussing the origin of carbonic inclusions. Laser Raman spectroscopy was used to determine the composition of the carbonic inclusions, and gas chromatography (GC) to quantify the volatile composition of fluid inclusions in bulk samples. He and Ar isotopes of bulk fluid inclusions were analyzed to study the origin of the fluids. Fluid phase separation modeling was carried out for different initial fluid compositions to evaluate the volumetric proportions of the coexisting immiscible liquid and vapor phases, and to determine how much water should have been present in the carbonic-rich inclusions if it had not been preferentially lost after entrapment. The origin of the $H_2O$-poor, $CO_2$-dominated fluid and its implications on gold transport are discussed.

## Regional and local geology

The Campbell-Red Lake gold deposit is located in the Red Lake greenstone belt, Superior Province, western Ontario, Canada. With a total of approximately 840 t of gold (past production + reserves) and an average grade of 21 g/t Au, the Campbell-Red Lake deposit is one of the largest and richest Archean gold deposits in Canada (Fig. 1), and belongs to a world-class (>100 t gold; see Poulsen et al. 2000) category. The Goldcorp High-grade Zone at the Red Lake mine (formerly known as the A.W. White and the Dickenson mines), one of the two mines currently exploiting the deposit (the other one is Campbell mine, Fig. 1), is characterized by very high gold grades, having produced more than 1.5 Moz at an

average grade of 88 g/t Au since the beginning of its exploitation in 2001 (Dubé et al. 2004).

The Red Lake greenstone belt consists of 2.99–2.89 Ga volcanic-dominated Mesoarchean rocks and 2.75–2.73 Ga Neoarchean volcanic rocks, which are separated by an angular unconformity (Sanborn-Barrie et al. 2001, 2004). Two main episodes of penetrative deformation ($D_1$, $D_2$) took place after the ca. 2.74 Ga volcanism (Sanborn-Barrie et al. 2001), resulting in two sets of folds ($F_1$, $F_2$) and associated foliation ($S_1$, $S_2$). $D_1$ deformation probably took place between 2,742 and 2,733 Ma and reflects an east-directed shortening, whereas $D_2$ deformation occurred between ca. 2,723 and 2,712 Ma in response to the Uchian phase of the Kenoran orogeny, which is related to the collision between the North Caribou terrane to the north of the Red Lake greenstone belt and the Winnipeg River terrane to the south (Dubé et al. 2004; Sanborn-Barrie et al. 2004). Post-collisional deformation ($D_3$) probably continued to about 2,700 Ma (Dubé et al. 2004; Sanborn-Barrie et al. 2004). $D_2$ is the most important deformation event in the Red Lake greenstone belt, and was synchronous with peak regional metamorphism and extensive granitic plutonism (Dubé et al. 2004; Sanborn-Barrie et al. 2004).

The Campbell-Red Lake gold deposit is hosted by volcanic rocks of the Mesoarchean Balmer Assemblage (ca. 2.99 Ga), which consists of tholeiitic and komatiitic basalts and peridotitic komatiites, with minor felsic volcanic and pyroclastic rocks, banded iron formation and clastic sedimentary rocks (Corfu and Andrews 1987; Sanborn-Barrie et al. 2001, 2004). The host rocks have been metamorphosed to middle greenschist and amphibolite facies (Damer 1997; Penczak and Mason 1997, 1999; Tarnocai 2000; Thompson 2003). The amphibolite–greenschist isograd occurs within the Campbell-Red Lake deposit (Mathieson and Hodgson 1984; Andrews et al. 1986; Damer 1997; Tarnocai 2000). The main structures in the deposit area, which formed during $D_2$, consist of a series of southeast-trending folds ($F_2$), as outlined by the geometry of the peridotitic komatiite (Fig. 1), and three southeast-trending, steeply-dipping (70–80°S) brittle-ductile structures known as the Campbell, Dickenson, and New Mine fault zones, which disrupt the folds (Fig. 1). A number of quartz feldspar porphyry (QFP) and feldspar porphyry (QP) dykes in the deposit area, ca. 2,714 to 2,712 Ma (Corfu and Andrews 1987; Dubé et al. 2004), crosscut $F_2$ folds (Fig. 1) and $S_2$ fabrics, and are overprinted by weakly to moderately developed $S_3$ foliation (Dubé et al. 2004). Lamprophyre dykes of 2,702 to 2,699 Ma (Dubé et al. 2004) are well developed in the deposit area (Fig. 1).

Gold mineralization at the Campbell-Red Lake deposit is mainly controlled by deformation zones along the "Red Lake Mine trend", which is a hydrothermal and structural corridor including the Campbell, Dickenson and New Mine fault zones (Fig. 1; Penczak and Mason 1997; Tarnocai 2000; Dubé et al. 2004). The deposit is divided into different "ore zones" (e.g., CUU, SC, ESC, etc. in Fig. 1). Extremely high-grade gold mineralization within the Goldcorp High Grade Zone (between levels 31 and 38, 1,350–1,700 m below surface) at the Red Lake mine is mainly located within or close to an $F_2$ antiform (Dubé et al. 2004). The deposit is characterized by numerous barren to low-grade banded colloform-crustiform carbonate (ankerite) ± quartz veins and cockade breccias (MacGeehan and Hodgson 1982; Penczak and Mason 1997, 1999; Tarnocai 2000; Dubé et al. 2004). Gold mineralization is mainly associated with arsenopyrite-rich silicic replacement of carbonate veins and breccias, as well as enclosing wall rock selvages, accompanied by variable amounts of pyrite, pyrrhotite, magnetite, and locally with trace amounts of sphalerite, chalcopyrite and stibnite (Twomey and McGibbon 2001; Dubé et al. 2004). Dubé et al. (2004) have presented several lines of evidence to show that extensive iron–carbonate veining is mainly a pre- to early-$D_2$ event, whereas the main-stage gold mineralization and associated arsenopyrite-rich silicification are mainly synchronous with $D_2$ deformation, regional tectono-metamorphism and magmatism. Both the main-stage gold mineralization and their host rocks are cut by the 2,714 – 2,712 Ma feldspar porphyry dykes and the 2,702–2,699 Ma lamprophyre dykes (Dubé et al. 2004). Minor late-stage gold mineralization occurs as visible gold coating fractures that cut the 2,702 Ma lamprophyre dykes, probably due to remobilization of the main-stage gold (Tarnocai 2000; Twomey and McGibbon 2001; Dubé et al. 2004).

The Balmer Assemblage rocks in the Red Lake greenstone belt have commonly been strongly altered. MacGeehan et al. (1982) has distinguished a "feldspar-destructive" alteration spatially associated with gold mineralization from a regional-scale spilitic alteration, and Parker (2000) differentiated a ferroan-dolomite alteration proximal to gold mineralization from a contemporaneous calcite alteration, which is widespread in the greenstone belt, both coeval with barren silicification and potassic alteration, and overprinted by mineralization-related silicification at the gold deposits. Penczak and Mason (1997, 1999) have divided the alteration in the mineralized zones at the Campbell mine into three phases, i.e., early alteration, main-stage vein-associated alteration, and mineralization-associated alteration. The early alteration consists of biotite alteration, carbonatization, silicification, and aluminous alteration, and is most intensely developed on major fault zones, whereas the main-stage vein-associated alteration is characterized by local carbonatization and chloritic selvages around colloform-crustiform carbonate-quartz veins, as well as distal chloritic alteration flanking and replacing inner biotite-carbonate-altered zones (Penczak and Mason 1997, 1999). The alteration associated with gold mineralization is characterized by silicification, with local development of quartz-sericite alteration (Penczak and Mason 1997, 1999). Penczak and Mason (1997, 1999) interpreted all the alteration phases as pre-penetrative deformation and pre-regional metamorphism events, and assigned the Campbell-Red Lake gold

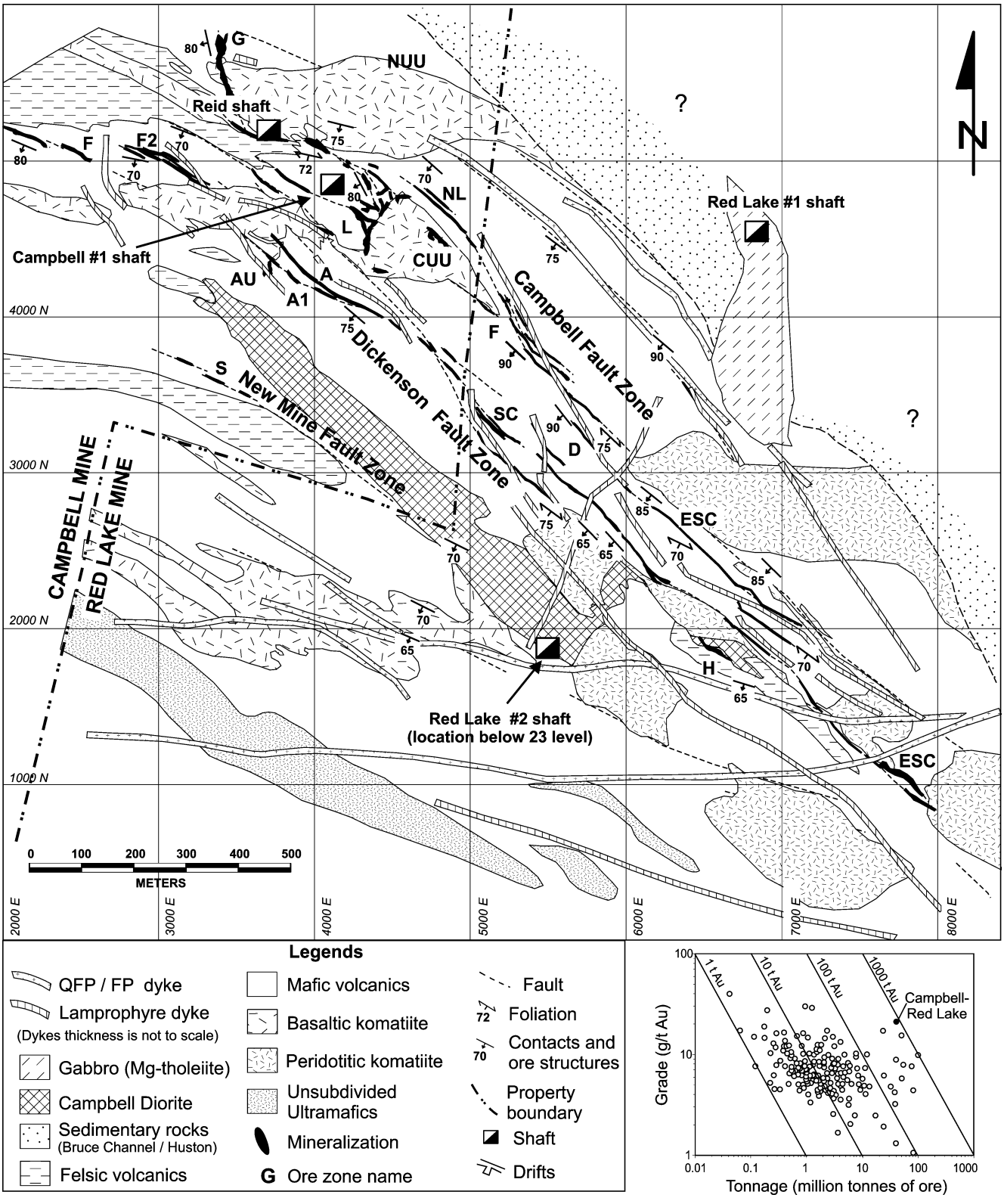


**Fig. 1** Geologic map of the Campbell-Red Lake gold deposit at level 15 (after Dubé et al. 2004; modified from Goldcorp geological data) and grade-tonnage plot of Canadian (Superior + Slave) Archean gold deposits (modified from Poulsen et al. 2000). The deposit is divided into the Campbell mine and the Red Lake mine, each consisting of a number of "ore zones" such as CUU, SC, ESC, etc

deposit to a deformed and metamorphosed low-sulfidation epithermal type, whereas Mathieson and Hodgson (1984) proposed that gold mineralization is syn-tectonic and syn-metamorphic, overprinting pre-metamorphic "feldspar-destructive" alteration. Twomey and McGibbon (2001) and Dubé et al. (2004) noted that a proximal centimetre- to metre-wide reddish-brown biotite-carbonate alteration with disseminated arsenopyrite, pyrite, pyrrhotite, and variable amounts of sericite, amphibole, and quartz in well foliated basalt is commonly associated with the silicified high-grade zones, and represents a key megascopic visual alteration vector to the high-grade mineralization at the Red Lake mine, suggesting that at least some biotite-carbonate alteration is directly related to gold mineralization. Tourmaline is a relatively late alteration product superimposed on other alteration and overprinting all deformation fabrics (Parker 2000; Dubé et al. 2004).

## Analytical methods

Fluid-inclusion microthermometry was carried out on a U.S.G.S.-style heating/freezing stage at the Geological Survey of Canada—Quebec Division and the University of Regina. The stages were calibrated with synthetic fluid inclusions of $H_2O$ (ice-melting temperature = 0°C; critical temperature = 374.1°C) and $H_2O$–$CO_2$ ($CO_2$-melting temperature = −56.6°C). The precision of the measurements of melting and homogenization temperatures of the carbonic phases are about ±0.2°C, whereas those of total homogenization temperatures of aqueous inclusions are around ±1°C.

The gas composition of individual carbonic fluid inclusions in quartz was analyzed using laser Raman microspectroscopy. The analyses were carried out at CREGU-UMR G2R, Nancy, France, with a LABRAM Jobin-Yvon system. The exciting radiation at 514.5 nm is provided by an ionized Argon laser (Spectra Physics). Detection limits are about 1 mol% for $CO_2$ and $N_2$ and 0.1 mol% for $CH_4$ and $H_2S$. The Raman spectrum of liquid water is very weak and thus cannot be obtained when water is not visible (Dubessy et al. 1992).

The gas composition of bulk fluid inclusions in separate minerals (ankerite and quartz) was analyzed using gas chromatography (GC) at McGill University, Montreal, Canada. Pure ankerite and quartz were separated by breaking sawn pieces of rock into small fragments and handpicking. The samples were rinsed six times with nanopure water (in beakers), allowed to stay in a bath of nanopure water at 40°C for 4 h, then dried for 3 h at 40°C, before being placed in the crushers. They were then heated to 120°C and flushed with UltraHighPurity (UHP) helium for 12 h, before being crushed. The gases released were delivered online to a GC (HP 5890) equipped with a megabore capillary column, using UHP helium as both the carrier and auxiliary gas, and were analyzed using a combination of photoionization and thermal conductivity detectors. The detection limits for various gas components range from $10^{-4}$ to $10^{-6}$ μmol (Salvi and Williams-Jones 2003).

He and Ar isotope compositions of bulk fluid inclusions in arsenopyrite and gold were analyzed at the Scottish Universities Environmental Research Centre. The minerals were separated at the Geological Survey of Canada, Ottawa, using a combination of crushing, sieve sizing and panning. The arsenopyrite separates were then passed through a 3.3 sg heavy liquid to remove composite sulfide-quartz (+gangue) grains. Magnetic grains were removed from each sample and contaminants visible under a binocular stereomicroscope were removed by handpicking prior to analysis. All samples were packed into stainless steel cups and crushed under ~1,000 psi in vacuo using an all metal hydraulic crusher. After purification of the extracted gases on hot and cold TiZr SAES getters, the heavy noble gases were trapped on liquid nitrogen-cooled charcoal. $^4$He and $^3$He were measured using a MAP215-50 magnetic sector mass spectrometer using procedures described by Stuart et al. (2000). Argon was released during He analysis and the Ar isotope composition was determined after evacuation of the He. All samples yielded $^4$He and $^{40}$Ar concentrations that were significantly in excess of blank concentrations. Helium isotope ratios were corrected for a 2–10% blank $^3$He. Blanks have $^{40}$Ar/$^{36}$Ar ratios that are indistinguishable from the atmospheric value (296). Since the Ar isotope data can most simply be interpreted as a mix of radiogenic and atmospheric Ar, no blank correction was applied.

## Petrography and fluid inclusion microthermometry

A total of 41 doubly polished thin sections (7 from the Campbell mine, 34 from the Red Lake mine) were examined for fluid inclusions. These samples were collected from the L zone (1851E Stope), DDH 31L042 (396.6–397 ft) and DDH 08L598 (469–469.2 ft) at the Campbell mine and the following veins or ore zones at the Red Lake mine: N–S breccia vein (level 31), a quartz-tourmaline vein in a lamprophyre dyke (level 34), HW zone (level 34), Main zone (level 34), HW/EW intersection (level 37), and HW5 zone (level 34–38). One additional sample from the Cochenour gold deposit, located at the northwest end of the Red Lake Mine trend, was also examined. Fluid inclusion types (carbonic, aqueous–carbonic, and aqueous) were visually classified for all samples, and microthermometry was carried out for 381 fluid inclusions from eight doubly polished thin sections, numbered Kg00-50-3, Kg00-50-4, Kg00-51A, Kg00-54, Kg00-11-1 (Red Lake mine), and Core-A2, Core-A3, and RP94-20A (Campbell mine). These samples are from carbonate veins with variable degrees of silicification and gold mineralization, and contain mineral phases from pre- and syn- to post-gold mineralization.

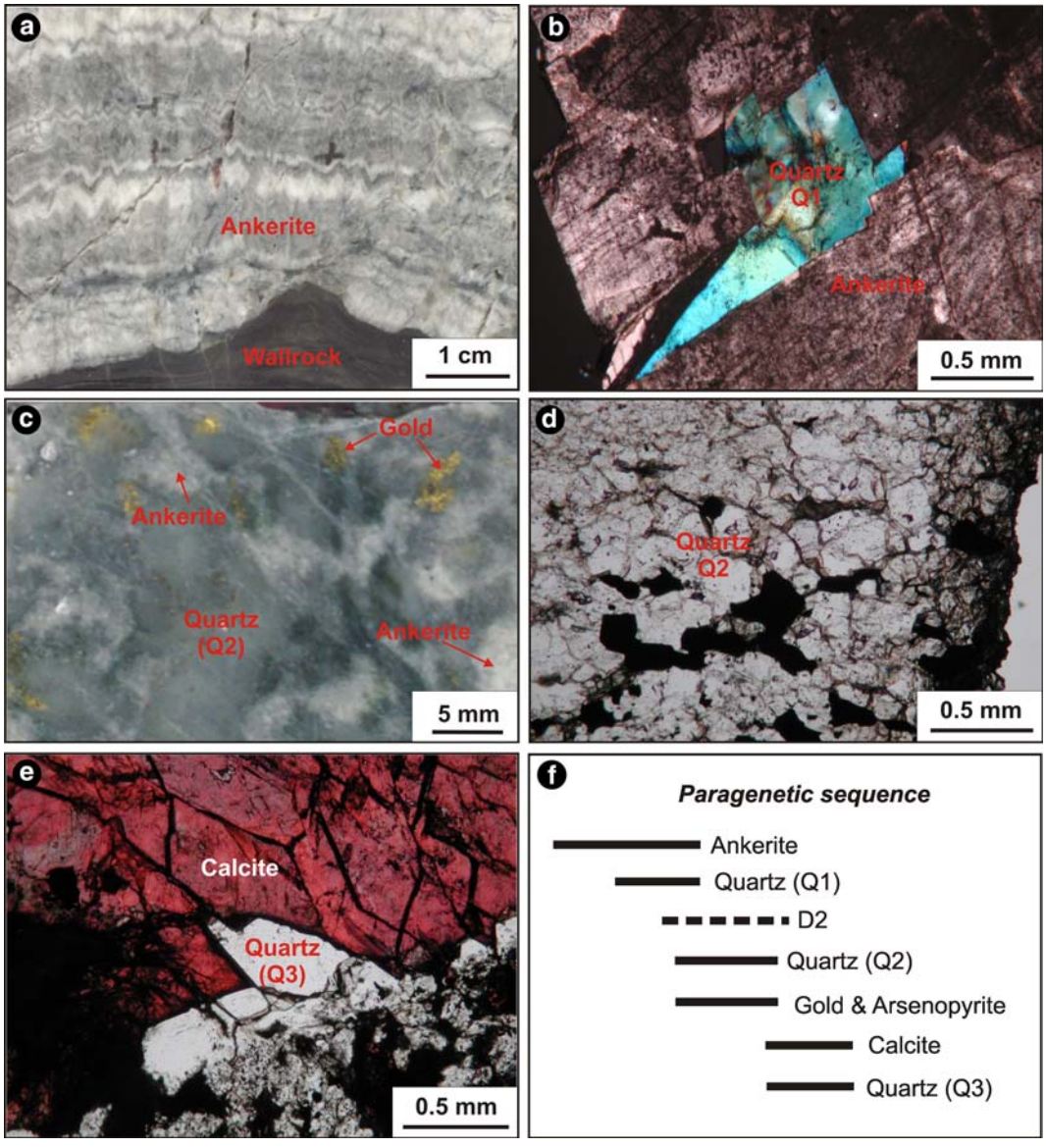


**Fig. 2** **a** Crustiform texture of ankerite vein. Sample KG00-50 (scanned rock slab). **b** An euhedral quartz crystal (Q1) showing growth contact with coarse, blocky ankerite crystals. Note the undulose interference color of the quartz related to deformation. Sample KG00-50-3 (cross polarized light). **c** Ankerite (*white*) replaced by fine-grained quartz (Q2) (*grey*) with associated gold. Sample KG00-11 (scanned rock slab). **d** Fine-grained quartz (Q2) associated with gold and sulfides. Sample KG00-11 (plane polarized light). **e** Euhedral quartz (Q3) associated with calcite in a vein cutting a lamprophyre dyke (plane polarized light; calcite is stained red by potassium ferricynaide-Arizarin Red S solution). **f** Paragenetic sequence of the gold-bearing carbonate-quartz veins

Ankerite was the first mineral to be precipitated in the veins. It locally shows a well-developed crustiform texture distinguished by a change in color from dark grey to white (Fig. 2a) and a cockade texture (Penczak and Mason 1997; Chi et al. 2002; Dubé et al. 2004). Some relatively large and locally euhedral quartz crystals (Q1) are associated with the ankerite (Fig. 2b). Most quartz (Q2), which is typically fine-grained, occurs as a replacement of ankerite, and is associated with arsenopyrite and native gold from the main stage gold mineralization (Figs. 2c, d). Late-stage quartz (Q3) occurs as euhedral crystals filling residual space left by ankerite and earlier quartz (Chi et al. 2002) or as fillings in fractures crosscutting lamprophyres, and is associated with calcite (Fig. 2e). The paragenetic sequence of the vein minerals is illustrated in Fig. 2f. Ankerite, Q1 and Q2 are commonly deformed to varying degrees as shown by undulose extinction and subgrain textures, whereas Q3 and calcite show little evidence of deformation.

In all the 41 samples examined, carbonic inclusions predominate, and in most doubly polished sections they are the only fluid inclusions observed. Rare aqueous and aqueous–carbonic inclusions were found in only a few samples, but in one of these samples (Kg00-51A), from a location where Q3 occurs in veins cutting lamprophyre, there are appreciable numbers of aqueous and aqueous–carbonic inclusions. Tarnocai (2000) also commented on the predominance of carbonic inclusions in the 36

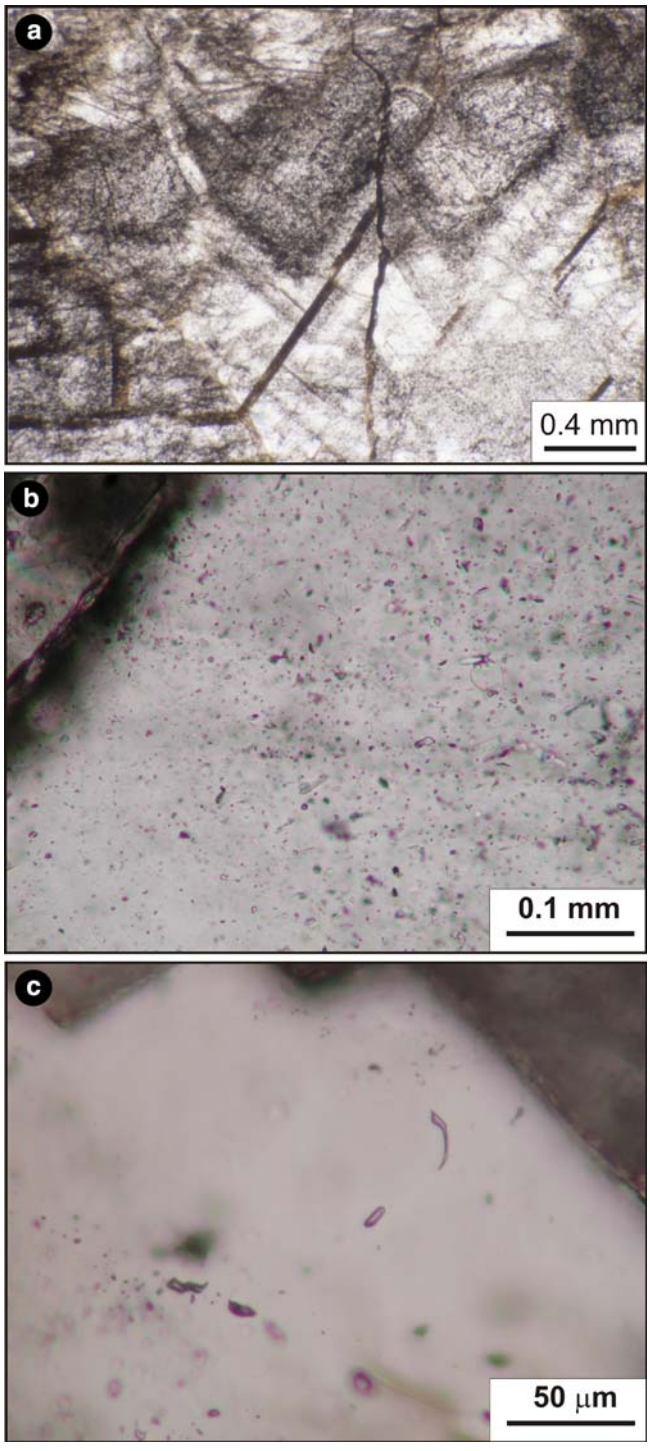


**Fig. 3** **a** Fluid inclusions distributed along growth zones in ankerite. Sample KG00-50-5 (plane polarized light). **b** Randomly distributed fluid inclusions in quartz (Q2). Sample Core-A2 (plane polarized light). **c** Isolated fluid inclusions in quartz (Q1). Sample KG00-50-3 (plane polarized light)

doubly polished sections that he examined from the Campbell mine, noting that aqueous–carbonic inclusions are only present in samples from a low Au-grade veinlet and represent a very small proportion of the fluid inclusions in these samples.

Fluid inclusions occur in healed fractures, clusters, or are isolated or randomly distributed in ankerite and quartz (Q1, Q2 and Q3). Well-defined primary inclusions are only found locally in ankerite where fluid inclusions are distributed in growth zones (Fig. 3a). Some of the growth zones are overprinted by healed fractures so that primary and secondary inclusions cannot be readily distinguished. Fluid inclusions randomly distributed in three dimensions (Fig. 3b) are likely primary, and the FIA concept is loosely applied to them by assuming that fluid inclusions occurring in a small volume in a crystal are penecontemporaneous. Isolated fluid inclusions (Fig. 3c) are also likely primary, and the validity of their microthermometric data is broadly constrained by comparison with neighboring fluid inclusions. Fluid inclusions occurring in clusters (Fig. 4) and short healed fractures (Fig. 5) (not including those in inter-granular healed fractures) are probably pseudosecondary, although a secondary origin cannot be ruled out, especially for those near grain boundaries. These fluid inclusions were likely entrapped contemporaneously and represent the most reliable and thus useful FIAs. The degree of consistency of microthermometric data of fluid inclusions within such FIAs provides a measure of the degree of modification of the inclusions after entrapment (Figs. 4, 5). Some FIAs show a considerable range of homogenization temperatures (Figs. 4b,c, 5e), which seem unrelated to the sizes of the fluid inclusions (Fig. 4b, c), whereas other FIAs show very consistent homogenization temperatures (Fig. 5a–d). In both cases, there is a systematic difference in homogenization temperatures among different FIAs within the same crystal (Figs. 4, 5).

The melting temperature of the carbonic phase ranges from −56.5 to −59.2°C for carbonic fluid inclusions from ankerite and different generations of quartz (Fig. 6), indicating that the fluids are dominated by $CO_2$, but contain trace to minor proportions of other gases. Fluid inclusions from Q1 and ankerite appear to have slightly higher $T_m$–$CO_2$ (mainly −56.6 to −57.3°C) (Fig. 6a) than those from the main ore-stage quartz (mainly −56.7 to −57.5°C) (Fig. 6b) and Q3 (mainly −57.2 to −58.0°C) (Fig. 6c).

The homogenization temperatures of $CO_2$ ($T_h$–$CO_2$) are highly variable among different FIAs (Fig. 7a), but show a relatively narrow range within individual FIAs (see Figs. 4, 5). $T_h$–$CO_2$ values in ankerite are relatively high (21–31°C), and some of them and many of those in associated quartz (Q1) homogenize to vapor (Fig. 7a). However, some of the fluid inclusions in Q1 have low $T_h$–$CO_2$ values (−5 to 20°C, to liquid) (Fig. 7a). Carbonic inclusions in Q2 have $T_h$–$CO_2$ values from 0 to 29°C, and generally homogenize to liquid (Fig. 7a), whereas the $T_h$–$CO_2$ values of carbonic inclusions in Q3 mainly fall in the range from 14 to 27°C (to liquid; Fig. 7a). Chi et al. (2003) discussed the significance of fluid pressure fluctuations indicated by the fluid inclusion data, and attributed them to periodic changes of pressure regime between supralithostatic and hydrostatic.

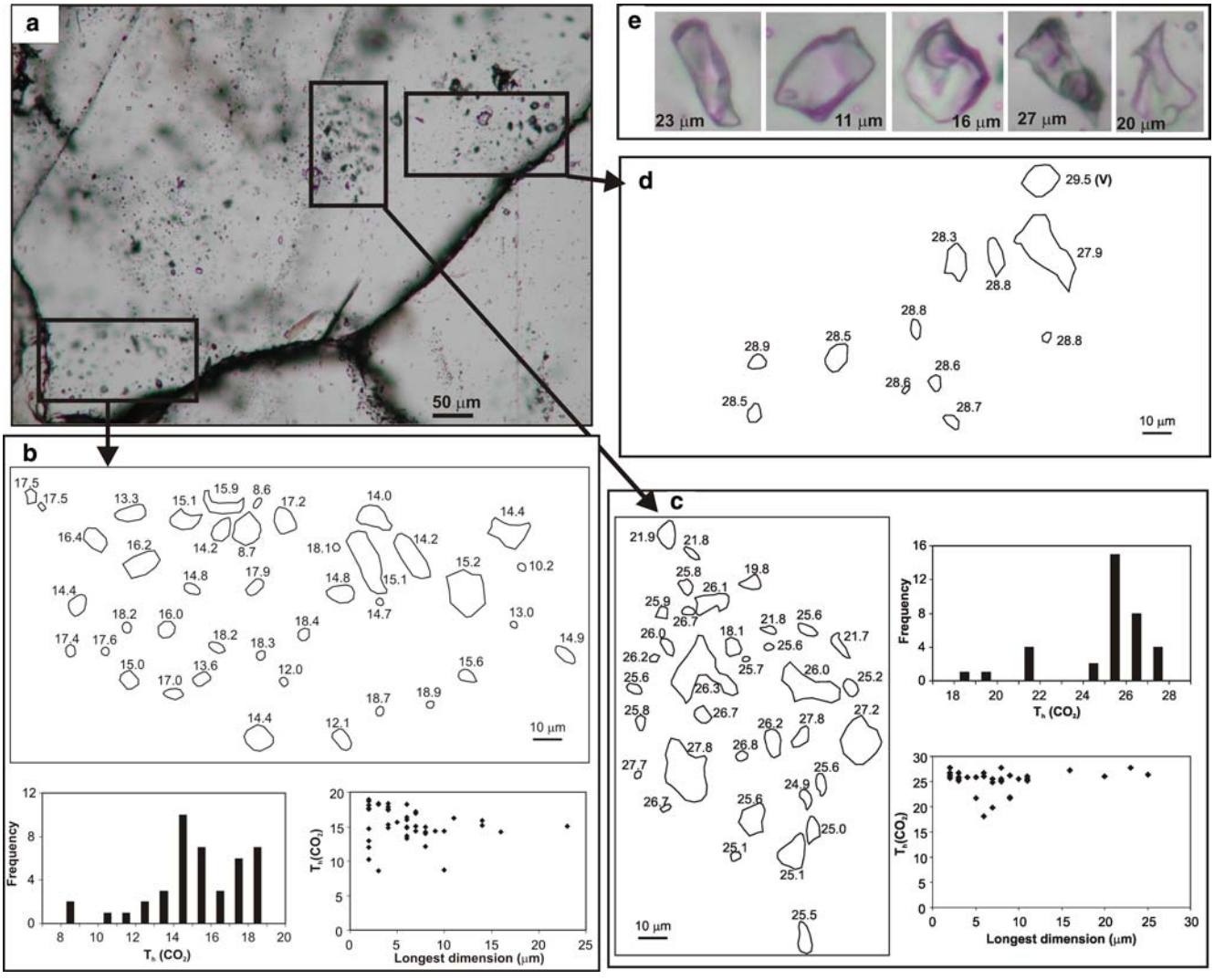


**Fig. 4** **a** Occurrence of fluid inclusions as "clusters" in a quartz crystal (Q2). The clusters appear to be controlled by short healed fractures. Sample Core-A3 (plane polarized light). **b** Distribution of carbonic inclusions within a cluster, histogram of their homogenization temperatures (to liquid), and relationship between homogenization temperatures and sizes (longest dimension). **c** Distribution of carbonic inclusions within another cluster, histogram of their homogenization temperatures (to liquid), and relationship between homogenization temperatures and sizes (longest dimension). **d** Distribution of carbonic inclusions within a cluster; note the consistency of homogenization temperatures (to liquid except one inclusion noted V in the upper right corner). **e** Enlargement of individual carbonic inclusions. Note there is no visible aqueous phase

Only a small number of aqueous fluid inclusions were observed in ankerite, Q1, and Q2, while more were found in Q3. The homogenization temperatures ($T_h$) of the aqueous inclusions range from 190 to 350°C in ankerite, 153 to 173°C in Q1, and 250 to 390°C in Q2 (Fig. 7b). Aqueous inclusions in Q3 have $T_h$ values ranging from 70 to 326°C (Fig. 7b), and many of them show high melting temperatures of clathrate (27.8–32.6°C).

## Gas composition of individual fluid inclusions

The gas compositions of individual carbonic fluid inclusions from five doubly polished sections (Red Lake mine: Kg00-50-5, Kg00-51A, Kg00-11-1; Campbell mine: Core-A3, and RP94-20A) were analyzed with laser Raman spectrometry (Fig. 8). The data indicate that the carbonic fluid inclusions are dominated by $CO_2$ in each of the three different generations of quartz, and have variable proportions of $CH_4$ and $N_2$. Most data for Q1 and Q3 lie on the $CO_2$–$CH_4$ binary system, whereas most data for Q2 are in the $CO_2$–$N_2$ system (Fig. 8). Two inclusions from Q2, phase changes of which were not observed during cooling, lie in the $CH_4$–$N_2$ binary system (Fig. 8). The average proportions (including all analyses) (mol%) of $CO_2$:$CH_4$:$N_2$ are 99.4:0.6:0 for Q1, 88.9:4.3:6.8 for Q2, and 97.5:2.2:0.3 for Q3. Trace amounts (< 0.1 mol%) of $H_2S$ were detected in several Q2 and Q3 inclusions.

The $H_2O$ peak was not observed in the carbonic inclusions examined.

## Bulk gas composition of fluid inclusions

Eight samples (7 ankerite and 1 quartz–Q2, Table 1), all from the Red Lake mine, were analyzed with gas chromatography (GC) to determine the composition of the bulk inclusion fluid. The results (Table 1) indicate that the fluids are dominated by $CO_2$, but contain significant amounts of $CH_4$ and minor $N_2$. There is no systematic difference among different samples, and the average proportions of $CO_2$:$CH_4$:$N_2$ (mol%) are 87.4:10.8:0.6. Trace amounts of $H_2S$ were detected, but not quantified. There was no significant difference between the height of the water peak for the blank (0.5 g Brazilian quartz, water-free) and those for the samples, indicating that the bulk fluid in all cases contained negligible $H_2O$. The much higher ratio of $CH_4$ to $N_2$ measured by GC compared to the average values obtained by laser Raman spectroscopic analyses of inclusions in Q2 indicates that although the overall fluid inclusion population is characterized by a predominance of $CH_4$ over $N_2$, individual inclusions may be enriched in $N_2$ (Fig. 8). This, in turn, suggests that there were multiple episodes of fluid trapping.

## He and Ar isotopes of bulk fluid inclusions

He and Ar isotope compositions of inclusion fluids in 5 arsenopyrite samples and 1 gold sample were analyzed (Table 2). Helium isotope ratios are normalized to the air ratio ($Ra = 1.39\times10^{-6}$). $^3He/^4He$ ratios (0.008–0.016 Ra) are comparable to crustal values (0.01–0.05 Ra), and significantly lower than mantle values (6–7 Ra). $^{40}Ar/^{36}Ar$ ratios (762.4–6119.0) are significantly higher than the atmospheric value (295.5), indicating the preservation of radiogenic $^{40}Ar$.

## Discussion

The data presented in this study clearly indicate that fluid inclusions in the Campbell-Red Lake gold deposit are predominantly carbonic. Laser Raman analysis does not show the $H_2O$ peak in carbonic inclusions, and GC analysis of bulk samples indicates that $H_2O$ is below the detection limit, confirming the extreme rarity of aqueous inclusions in ankerite and early and main ore-stage quartz (Q1, Q2). Questions that arise from these observations include: (1) do carbonic inclusions result from preferential leakage of water from aqueous–carbonic inclusions after entrapment or do they represent entrapment of a carbonic fluid? (2) does the rare

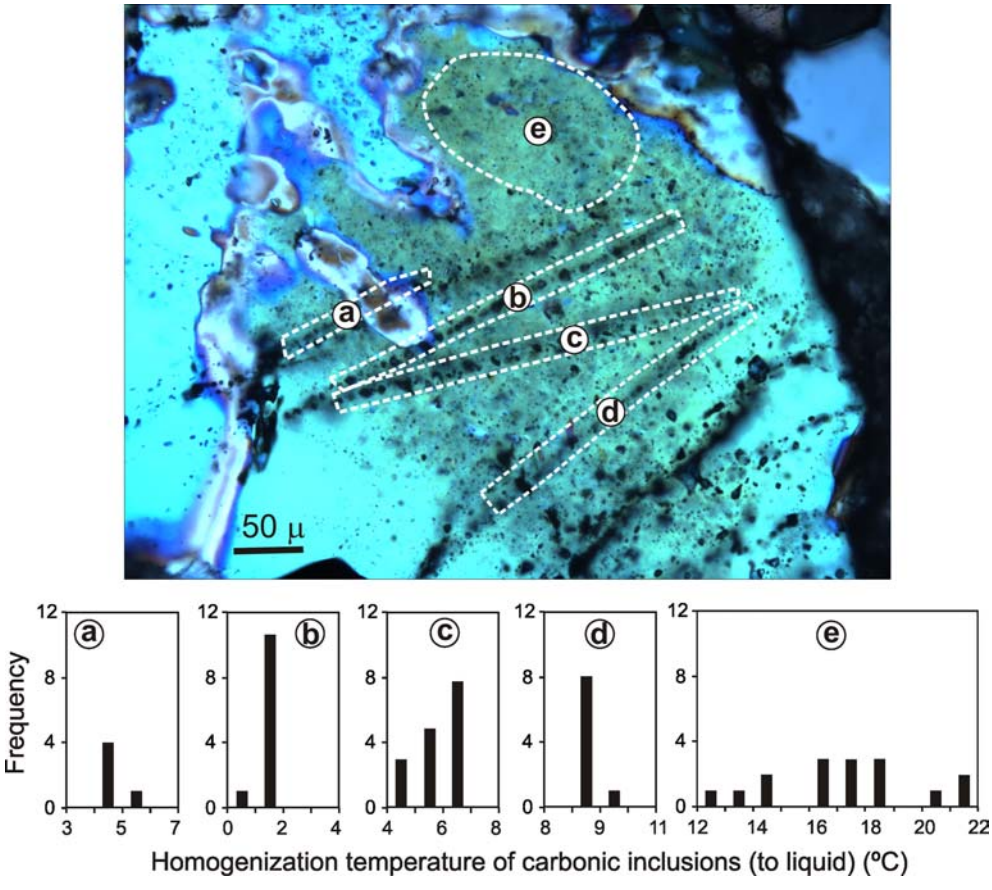


**Fig. 5** Photomicrographs showing carbonic fluid inclusions in short healed fractures (**a**, **b**, **c**, **d**) and randomly distributed (**e**) in quartz (Q1) (Sample KG00-54A; cross polarized light), and histograms of homogenization temperatures (to liquid) in individual fluid inclusions assemblages. Note the consistency of homogenization temperatures within individual healed fractures and the wide range for randomly distributed ones

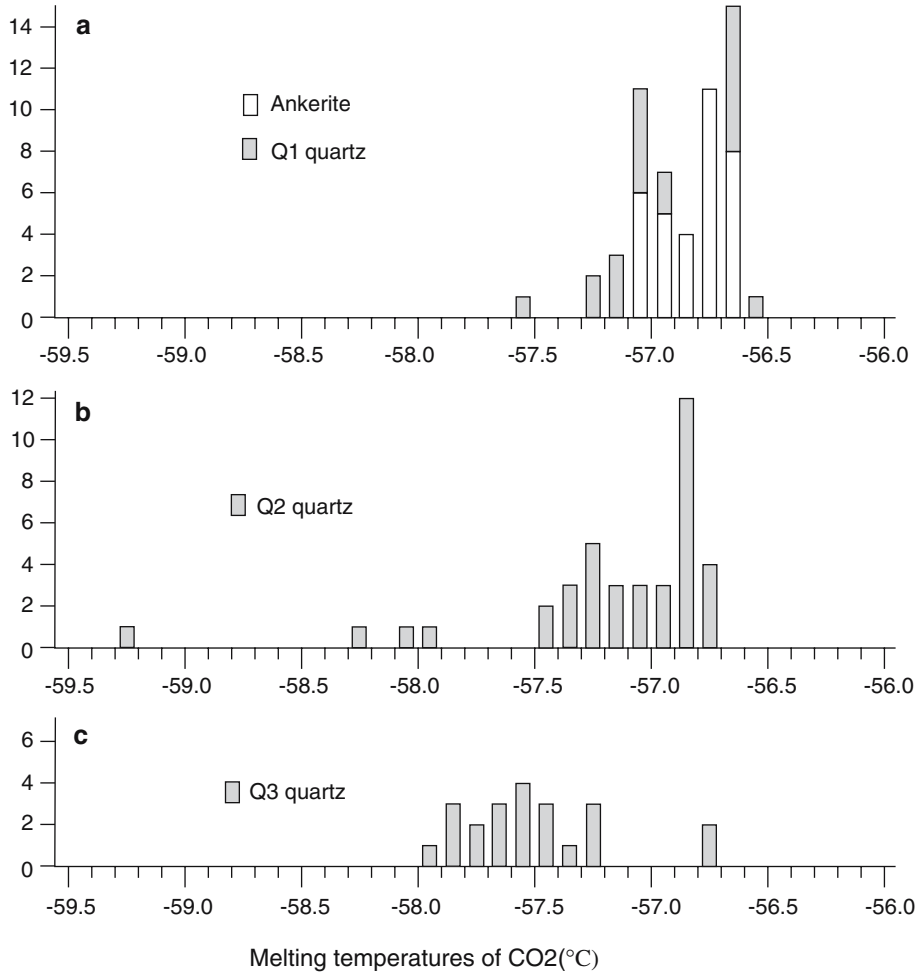


**Fig. 6** Histograms of melting temperatures of $CO_2$ of carbonic fluid inclusions. **a** ankerite and associated quartz (Q1). **b** Ore-stage quartz (Q2). **c** Post-mineralization quartz (Q3). Data from Chi et al. (2002, 2003)

occurrence of aqueous inclusions result from preferential entrapment of a carbonic phase over an aqueous phase produced by fluid unmixing or does it indicate that the carbonic fluid was not accompanied by an aqueous phase? and (3) if the fluid was initially poor in water, how did it transport silica and gold and alter the wall rocks? Similar questions have been asked and discussed in studies of the other gold deposits dominated by carbonic inclusions (e.g., Garba and Akande 1992; Schmidt Mumm et al. 1997, 1998; Klemd 1998; Xavier and Foster 1999; Wille and Klemd 2004). We further investigate these questions below based on the data from Campbell-Red Lake, emphasizing the use of the fluid inclusion assemblage (FIA) concept, quantitative modeling of phase separation, and comparison with other gold deposits.

## Entrapment of a carbonic fluid versus post-trapping leakage models

Whether or not the carbonic inclusions which dominate in some orogenic gold deposits were produced by preferential leakage of $H_2O$ from former aqueous–carbonic inclusions has been a controversial topic. A number of studies (e.g. Hollister 1990; Bakker and Jansen 1994; Johnson and Hollister 1995) have shown that $H_2O$ is preferentially lost over carbonic components when fluid inclusions are stretched after entrapment or the host mineral is deformed or recrystallized. This mechanism has been used to explain the origin of carbonic inclusions in high-grade metamorphic rocks (Hollister 1988, 1990), and has been argued to be responsible for the formation of carbonic inclusions in some gold deposits in the Ashanti Belt (Klemd 1998). Most researchers who have studied fluid inclusions in gold deposits dominated by carbonic fluid inclusions (e.g., Garba and Akande 1992; Schmidt Mumm et al. 1997, 1998; Xavier and Foster 1999), however, concluded that the carbonic inclusions represent a carbonic fluid that was $H_2O$-poor, at the time of entrapment. It is notable that these gold deposits dominated by carbonic inclusions are apparently not different from other gold deposits in terms of degree of metamorphism of the host rocks (green schist to amphibolite facies), timing of mineralization (syn- to post-peak metamorphism and deformation) and controlling structures (brittle-ductile shear zones and brittle faults) (Garba and Akande 1992; Schmidt Mumm et al. 1997, 1998; Xavier and Foster 1999), therefore, it is difficult to explain why the preferential $H_2O$-leakage

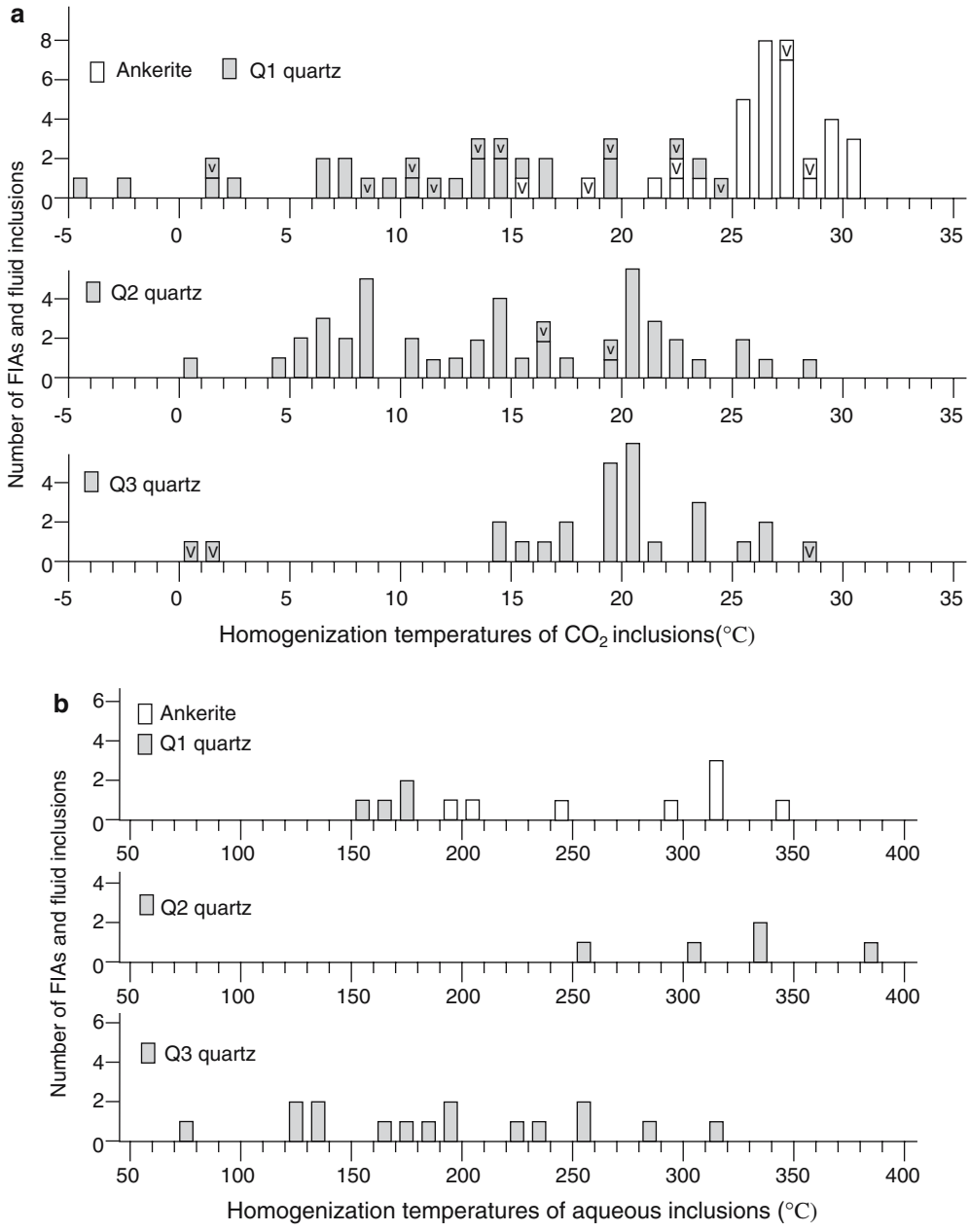


**Fig. 7** Histograms of homogenization temperatures of $CO_2$ fluid inclusions (**a**) and aqueous inclusions (**b**) "V" means homogenization to vapor. Data from Chi et al. (2002, 2003) and this study

process almost completely removed $H_2O$ from the $H_2O$–$CO_2$ inclusions in some deposits but did not do the same for other deposits. It is more likely that the processes controlling this difference in fluid inclusion populations lies outside the deposits, and is unrelated to the metamorphic and structural conditions at the sites of mineralization.

We support the hypothesis that the carbonic fluid inclusions represent a carbonic fluid present during carbonate veining and gold mineralization at the Campbell-Red Lake gold deposit with detailed FIA analysis. Fluid inclusions within a single FIA should have the same homogenization temperature if they have not been modified after entrapment (Goldstein and Reynolds 1994), excluding heterogeneous trapping. If fluid inclusions in an FIA are subject to modification after entrapment, their specific volumes will be changed to variable degrees depending on the size and shape of individual inclusions (Bodnar 2003), which will be reflected by the variation of homogenization temperatures of fluid inclusions within the FIA. The vulnerability of fluid inclusions to post-trapping modification is also related to the softness of the host minerals (Bodnar 2003), thus fluid inclusions in quartz (Mohs hardness = 7) are less prone to post-trapping modification than those in ankerite (Mohs hardness = 3.5–4). Given the deformation features of the mineralized zones at Campbell-Red Lake, it is reasonable to assume that many fluid inclusions may have been modified to varying degrees by post-trapping processes. If the fluid

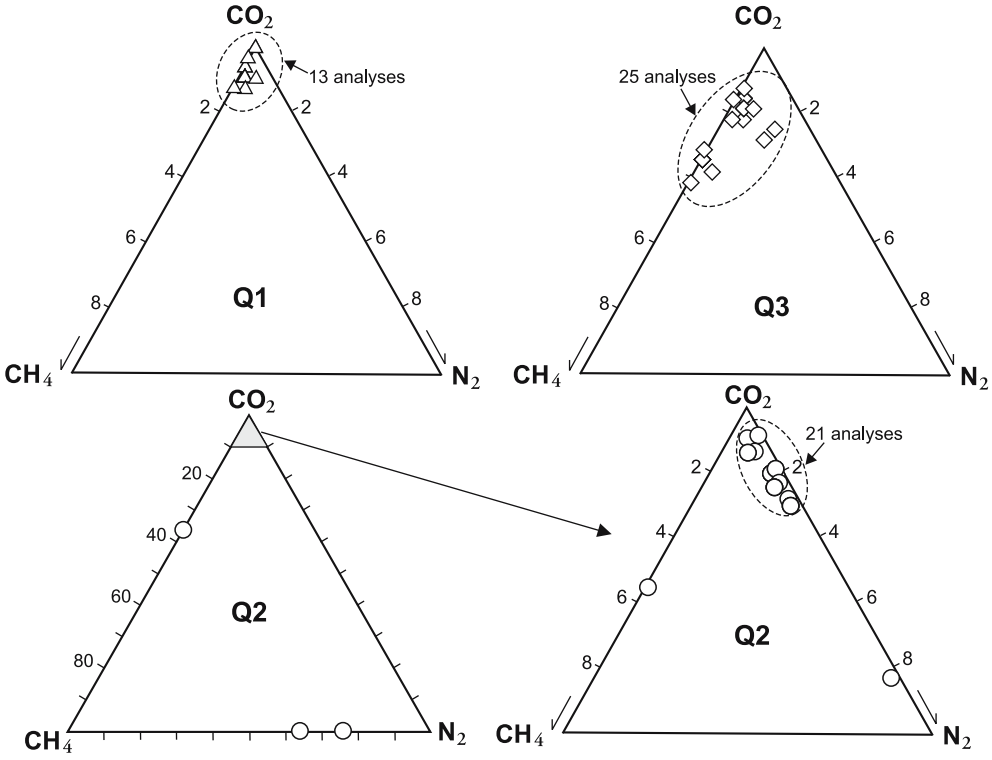


**Fig. 8** The $CO_2$–$CH_4$–$N_2$ composition (mol%) of carbonic fluid inclusions from different generations of quartz, as analyzed by laser Raman microspectrometry. Trace amounts (< 0.1 mol%) of $H_2S$ were detected in most of the inclusions from Q1 and Q2, and are not presented in the figure. Data from Chi et al. (2003) and this study

inclusions were originally composed of aqueous and carbonic components, we would expect to see variable proportions of an aqueous phase in the fluid inclusions depending on the degree of modification to which they have been subjected. Thus, we would expect to see more carbonic inclusions in ankerite than in quartz, and FIAs that show more variable homogenization temperatures would have more variable aqueous/carbonic ratios, whereas FIAs that have narrow homogenization temperature ranges would be composed most consistently of aqueous and carbonic phases. Our observations indicate that fluid inclusions in quartz and ankerite are both carbonic, and those in FIAs with highly convergent $T_h$ values (Figs. 4, 5) are also carbonic, free of any detectable water. These observations argue strongly against preferential $H_2O$ leakage as the principal mechanism of formation of carbonic inclusions in the Campbell-Red Lake deposit.

## Single carbonic fluid versus fluid unmixing models

If the carbonic fluid inclusions do not result from post-trapping modification, they may represent either a single carbonic fluid or the carbonic phase preferentially entrapped from coexisting, immiscible aqueous and carbonic fluids resulting from fluid unmixing. The single fluid model was proposed by Schmidt Mumm et al. (1997) and Xavier and Foster (1999) for the Ashanti and Fazenda Maria Preta gold deposits, respectively, and the fluid unmixing model was favored by Garba and Akande (1992) and Tarnocai (2000) for the Bin Yauri and Campbell-Red Lake gold deposits, respectively. Each model has some advantages over the other, but also faces some unsolved problems, which are discussed below.

The single fluid model readily explains the absence or extreme rarity of aqueous inclusions. However, the relationship between this water-poor fluid and hydrous alterations is unclear. At the Ashanti deposit, it has been observed that the intensity of chloritization, sericitization and epidotization increases toward quartz veins (Klemd 1998), and that carbonatization is very limited around the mineralized veins (Schmidt Mumm et al. 1997). Klemd (1998) interpreted the hydrous alteration as an indication of the passage of aqueous-bearing mineralizing fluids, whereas Schmidt Mumm et al. (1998) argued that these alteration types may have

**Table 1** Gas composition of bulk fluid inclusions analyzed by gas chromatography (mol%)

| Sample mineral | KG00-50-2a ankerite | 2b ank | 3a ank | 3b ank | 5a Ank | 5b ank | 6a quartz (Q2) | 7 ank | Average |
|---|---|---|---|---|---|---|---|---|---|
| $N_2$ | 0.5 | 0.7 | 0.9 | 0.6 | 0.6 | 0.8 | 0.3 | 0.3 | 0.6 |
| $CH_4$ | 10.4 | 12.0 | 16.9 | 14.2 | 13.4 | 15.1 | 8.0 | 6.3 | 12.0 |
| $CO_2$ | 89.1 | 87.3 | 82.2 | 85.2 | 86.0 | 84.1 | 91.7 | 93.4 | 87.4 |
| $H_2O$ | Negligible | Nl | Nl | Nl | Nl | Nl | Nl | Nl | Nl |

**Table 2** He and Ar isotopes of fluid inclusions

| Sample | Mineral | $^{3}He/^{4}He$ (Ra) | $^{40}Ar/^{36}Ar$ |
|---|---|---|---|
| KG01-28B | Arsenopyrite | 0.010 | 2095.5 |
| KG01-28A | Arsenopyrite | 0.011 | 3025.4 |
| KG01-39A | Arsenopyrite | 0.008 | 4370.9 |
| KG00-19A | Arsenopyrite | 0.008 | 4329.9 |
| KG02-73D-As | Arsenopyrite | 0.010 | 6119.0 |
| KG02-73D-Au | Gold | 0.016 | 762.4 |

resulted from aqueous fluids unrelated to mineralization. The limited distribution of carbonatization was interpreted to reflect restricted migration of the carbonic fluid along discrete shear zones and limited contact between the fluid and wall rocks (Schmidt Mumm et al. 1997). At the Campbell-Red Lake deposit, mineralized zones are characterized by a proximal biotite-carbonate alteration (Twomey and McGibbon 2001; Dubé et al. 2004). At the Campbell mine, the biotite-rich alteration is flanked and replaced by chloritic alteration (Penczak and Mason 1997, 1999). This alteration pattern does not seem to be incompatible with the single carbonic fluid model if the host rocks were subjected to extensive hydrothermal alteration prior to carbonate veining and gold mineralization, as originally proposed by MacGeehan and Hodgson (1982) and MacGeehan et al. (1982). In such a model, water for biotitization, chloritization and sericitization may have been locally derived from the host rocks, which had been previously hydrolyzed, rather than from the mineralizing fluids.

Because gold is invariably associated with silicification (Q2) and fluid inclusions (primary and pseudosecondary) in Q2 are carbonic, the single carbonic fluid model would imply that both gold and silica were transported by the $CO_2$-dominated fluids. Thermodynamic analysis suggests that the solute species of Si in a $CO_2$–$H_2O$ fluid is $H_4SiO_4$ (Newton and Manning 2000) or $Si(OH)_4.2H_2O$ (Walther and Orville 1983), and experiments indicate that the solubility of $SiO_2$ decreases with decreasing $X_{H_2O}$ (Walther and Orville 1983; Newton and Manning 2000). No experimental data are available on $SiO_2$ solubility in a water-free carbonic fluid, and it is not known what solute species Si may form in such a fluid. The gold-transporting ability of carbonic fluids is also unknown. However, there is a general consensus that gold is transported primarily as bisulfide and chloride complexes in aqueous fluids at elevated temperatures (Gammons and Williams-Jones 1997; Benning and Seward 1996). Both laser Raman and GC analyses of fluid inclusions from Campbell-Red Lake indicate that $H_2S$ was present in the ore fluid, and it is therefore attractive to speculate that complexation of gold with this species was the means by which gold was transported in the ore fluid. Although there are no experimental data on the solubility of gold in an $H_2S$-bearing fluid, this hypothesis is supported by experimental findings that $H_2S$ gas can dissolve appreciable concentrations of other metals, e.g., Sb (Zakaznova-Iakoleva et al. 2001). We therefore propose, as documented for Sb, that the gold at Campbell-Red Lake was transported as an $H_2S$-solvated species having the stoichiometry $Au.n(H_2S)^{gas}$, and that its solubility depended only on the fugacity of $H_2S$ and not on whether the latter was dissolved in $H_2O$ or $CO_2$.

The fluid unmixing model has several advantages over the single carbonic fluid model, although the scarcity of aqueous inclusions and the lack of any unequivocal petrographic evidence of two coexisting carbonic and aqueous phases make it difficult to validate the model. The most obvious advantage of the model is that it readily explains the hydrous alteration and the transportation of silica and gold, as the mineralizing fluid is assumed to be composed of aqueous and carbonic components like that in most orogenic gold deposit. In addition, fluid unmixing has been proposed as a major mechanism of gold deposition in orogenic gold deposits (e.g., Robert and Kelly 1987; Naden and Shepherd 1989; Guha et al. 1991). The question that this model does not answer is why fluid inclusion evidence of the aqueous phase is absent or extremely rare.

The interpretation that the carbonic phase is preferentially trapped due to its higher wetting angles than aqueous phase (Watson and Brenan 1987) is not sufficient, because the same mechanism can be applied to other gold deposits where fluid unmixing is well-documented, and yet aqueous and aqueous–carbonic inclusions are commonly recorded. Little is known about the relationship between the volume ratio of carbonic to aqueous phase in the immiscible fluids and the ratio of carbonic to aqueous inclusions being entrapped. We believe that if the fluid unmixing model were to be applicable to deposits dominated by carbonic fluid inclusions, the pre-unmixing fluid would be significantly more enriched in carbonic species than in ordinary orogenic gold deposits, such that the vapor resulting from phase separation would be volumetrically predominant and the trapping of the aqueous phase prevented.

Using the "GeoFluids" program (from the website of UCSD-Chemical Geology Group: http://www.geotherm.ucsd.edu/geofluids), which is based on the equation of state of Duan et al. (1995) for the $H_2O$–$CO_2$–NaCl system, the volume ratios of carbonic to aqueous phase in the immiscible fluids resulting from phase separation of four different initial fluids and the $X_{H_2O}$ values in the vapor were calculated. Fluid $a$($X_{H_2O}$ = 0.9, $X_{CO_2}$ = 0.07, $X_{NaCl}$ = 0.03) and $c$ ($X_{H_2O}$ = 0.48, $X_{CO_2}$ = 0.48, $X_{NaCl}$ = 0.04) represent the minimum and maximum $X_{CO_2}$ values for the "majority of orogenic gold deposits", and fluid $b$ ($X_{H_2O}$ = 0.8, $X_{CO_2}$ = 0.16, $X_{NaCl}$ = 0.04) is the average of the "most frequently recorded composition" of orogenic gold deposits (Ridley and Diamond 2000), whereas fluid $d$ ($X_{H_2O}$ = 0.16, $X_{CO_2}$ = 0.80, $X_{NaCl}$ = 0.04) represents a fluid much more enriched in $CO_2$ than in most orogenic gold deposits. The results of the simulation indicate that when the initial fluids are dominated by $H_2O$ (fluids $a$ and $b$), the liquid phase resulting

from phase separation is volumetrically more important (52–79%) than the vapor, and the vapor contains significant amounts of $H_2O$. When the initial fluid contains equal amounts of $H_2O$ and $CO_2$ (fluid *c*), the volume of the vapor produced by phase separation (57–96%) is greater than the liquid, and the $X_{H_2O}$ values in the vapor range from 0.22 to 0.47. When the initial fluid is significantly enriched in $CO_2$ (fluid *d*), the vapor produced by phase separation is volumetrically dominant (94–97%), and the $X_{H_2O}$ values in the vapor range from 0 to 0.15. We conclude that phase separation from a fluid with composition *a*, *b* or *c* cannot produce a volumetrically dominant carbonic fluid phase, whereas a fluid with pre-unmixing $X_{CO_2} > 0.8$ may give rise to a carbonic phase, the volume of which is so overwhelmingly greater than the liquid phase that the latter cannot be entrapped.

### Source of the $H_2O$-poor, $CO_2$-dominant fluids

As is evident from the above discussion, both the single carbonic fluid and the fluid unmixing models imply an initial fluid dominated by carbonic components and poor in water. The $H_2O/CO_2$ ratio in the crust is about 40 on a global scale (Fyfe et al. 1978), so the average fluid in the crust is dominated by water, and the formation of a fluid dominated by carbonic components requires some special and localized geologic processes or environments where carbonic components are significantly enriched relative to water. In addition, the fluid must be focused along discrete structures so that it is not "diluted" by fluids from the environment dominated by water.

Considering that the main gold mineralization stage at Campbell-Red Lake was synchronous with regional tectono-metamorphism and magmatism (Dubé et al. 2004), the ore-forming fluids are possibly of metamorphic or magmatic origin. Carbonic inclusions are common in high-grade metamorphic rocks (Touret 2001) and in mantle xenoliths (Anderson and Neumann 2001). The $H_2O$-poor, carbonic fluid may have been derived from the lower crust, with or without input from the mantle. Enrichment of $CO_2$ in the lower crust during granulitization may have resulted from an influx of $CO_2$ from the mantle (Newton et al. 1980; Santosh 1986), or from preferential $H_2O$ removal by partial melting accompanying granulitization (Fyon et al. 1989; Sarkar et al. 2003). Although the noble gas isotope data for the Campbell-Red Lake deposit do not show a mantle signature, some contribution from the mantle cannot be ruled out because although we have argued that the formation and predominance of carbonic inclusions did not result from post-trapping modification, most of the fluid inclusions have likely experienced variable degrees of post-trapping modification, and the influence of these changes on the He isotopes of the inclusion fluids is unknown. The $H_2O$-poor, carbonic fluid at the Campbell-Red Lake gold deposit may also have been derived from degassing of magmatic intrusions. In most cases, felsic magmas generated in the crust are enriched in $H_2O$, but there are examples showing $CO_2$ dominance in ultrahigh-temperature granitoids (Santosh et al. 2005), although this kind of granitic magma may not be able to migrate too far from the source region because it will solidify rapidly. Alternatively, if the magma initially contains both $H_2O$ and $CO_2$, and intrudes into higher levels of the crust, $CO_2$-dominated fluids may be derived from preferential $CO_2$ release during the early stage of magmatic degassing (Lowenstein 2001). Such a possibility may be evaluated by studying fluid inclusions in a regional scale, especially those in the syn-mineralization granitic intrusions (Dubé et al. 2004).

A final potential origin of the $CO_2$-dominated fluid is that it represents the vapor resulting from fluid phase separation below the site of mineralization (Chi et al. 2003, 2005). Although it has been proposed by a number of studies that fluid unmixing causes gold precipitation (e.g., Robert and Kelly 1987; Naden and Shepherd 1989; Guha et al. 1991), contrary examples exist and indicate that fluid unmixing does not necessarily result in gold precipitation (see Mikucki 1998). Even if certain amounts of gold are extracted from the fluid system during unmixing, it is still possible that large amounts of gold are partitioned into the vapor, and carried by $H_2S$ which is partitioned preferentially into the vapor during phase separation (Naden and Shepherd 1989; Gammons and Williams-Jones 1997). Moreover, Heinrich et al. (1999) have shown that Au, Cu, As and B tend to be selectively partitioned into the vapor of boiling magmatic fluid systems. Thus, although much of the Cu in porphyry–epithermal systems is precipitated to form a porphyry copper deposit due to the temperature drop that attends boiling, large amounts of Cu and Au are transported in the vapor to form epithermal deposits at higher levels (Williams-Jones et al. 2005).

## Conclusions

The data from fluid inclusion microthermometry, laser Raman spectrometry and gas chromatography indicate that fluid inclusions in the ankerite veins and main ore-stage quartz from the Campbell-Red Lake gold deposit are predominantly carbonic, composed mainly of $CO_2$, with minor $CH_4$ and $N_2$, and trace $H_2S$. Aqueous inclusions are extremely rare. Fluid inclusion assemblage analysis suggests that although post-trapping modifications and host mineral deformation may have altered the inclusions to varying degrees, these processes were not solely responsible for the formation of carbonic fluid inclusions and the extreme rarity of aqueous inclusions. The carbonic inclusions most likely represent a primary fluid present during carbonate veining and gold mineralization at Campbell-Red Lake, and this fluid may have been derived either from phase separation of an initial aqueous–carbonic fluid or from a single carbonic fluid. In the case of fluid phase separation, the pre-separation

fluid is likely to have been significantly enriched in $CO_2$ (with $X_{CO_2} > 0.8$) in order to produce the $CO_2$-dominated fluid and to prevent the entrapment of the aqueous fluid. The $CO_2$-enriched fluid may have been derived from the lower crust in relation to granulitization or from early degassing of magmatic intrusions. If the initial fluid contains some water (fluid phase separation model), gold may have been carried as gold bisulfide complexes as in most orogenic gold deposits, whereas if the initial fluid was free of water (the single carbonic fluid model), gold may have been transported as $H_2S$-solvated species.

**Acknowledgements** Financial support from the Geological Survey of Canada (GSC) (Dubé; and contributions to Chi) and NSERC (Chi and Williams-Jones) are acknowledged. We would like to thank Finley Stuart of Scottish Universities Environmental Research Centre for He and Ar isotope analysis, Michael S.J. Mlynarczyk (McGill University) for GC analysis, and Therese Lhomme (CREGU -UMR G2R, Nancy, France) for laser Raman analysis. Thanks to M. Burns, I. Jonasson and I. Bilot of the GSC for the preparation of the arsenopyrite and gold concentrates. The staff of Goldcorp Inc., in particular Gilles Filion, Stephen McGibbon, Rob Penczak, Tim Twomey, John Kovala, Mark Epp and Michael Dehn are thanked for their scientific contribution, logistic and financial support. Rob Penczak is especially thanked for sharing his knowledge of the entire Campbell-Red Lake deposit and for providing some of the samples included in this study. Jayanta Guha, Michel Malo, Mary Sanborn-Barrie, Tom Skulski, Jack Parker, François Robert, Howard Poulsen, Vic Wall and Matt Ball are thanked for constructive discussions. Finally, we would like to thank Larry Meinert, Ronald Bakker, Phillip Brown and Georges Beaudoin for their detailed review of the manuscript, which has greatly improved the quality of the paper.

## References

Anderson T, Neumann E-R (2001) Fluid inclusions in mantle xenoliths. Lithos 55:301–320

Andrews AJ, Hugon H, Durocher M, Corfu F, Lavigne M Jr (1986) The anatomy of a gold-bearing greenstone belt: Red Lake, northwestern Ontario, Canada. In: MacDonald AJ (ed) Proceedings of Gold '86, an international symposium on the geology of gold, Toronto, Canada, pp 3–22

Baker T (2002) Emplacement depth and carbon dioxide-rich fluid inclusions in intrusion-related gold deposits. Econ Geol 97:1111–1118

Bakker RJ, Jansen JBH (1994) A mechanism for preferential $H_2O$ leakage from fluid inclusion in quartz, based on TEM observations. Contrib Mineral Petrol 116:7–20

Benning LG, Seward TM (1996) Hydrosulphide complexing of Au(I) in hydrothermal solutions from 150–400 degrees C and 500–1500 bar. Geochim Cosmochim Acta 60:1849–1871

Bodnar RJ (2003) Reequilibrium of fluid inclusions. In: Samson I, Anderson A, Marshall D (eds) Fluid Inclusions: analysis and interpretation. Mineralogical Association of Canada Short Course Series 32:213–231

Chi G, Dubé B, Williamson K (2002) Preliminary fluid-inclusion microthermometry study of fluid evolution and temperature–pressure conditions in the Goldcorp High-Grade zone, Red Lake mine, Ontario. Geological Survey of Canada, Current Research, 2002-C27, 12 p

Chi G, Dubé B, Williamson K (2003) Fluid evolution and pressure regimes in the Red Lake Mine Trend: fluid-inclusion evidence for a protracted, highly dynamic hydrothermal system. Geological Survey of Canada, Current Research, 2003-C28, 16 p

Chi G, Williams-Jones AE, Dubé B, Williamson K (2005) Carbonic vapor-dominated fluid systems in orogenic-type Au deposits. Geochim Cosmochim Acta 69:A738

Corfu F, Andrews AJ (1987) Geochronological constraints on the timing of magmatism, deformation, and gold mineralization in the Red Lake greenstone belt, northwestern Ontario. Can J Earth Sci 24:1302–1320

Damer DC (1997) Metamorphism of hydrothermal alteration at the Red Lake Mine, Balmertown, Ontario. Unpublished Master thesis, Queen's University, 195p

Duan Z, Moller N, Weare JH (1995) Equation of state for the $NaCl–H_2O–CO_2$ system: prediction of phase equilibria and volumetric properties. Geochim Cosmochim Acta 59:2869–2882

Dubé B, Williamson K, McNicoll V, Malo M, Skulski T, Twomey T, Sanborn-Barrie M (2004) Timing of gold mineralization in the Red Lake gold camp, northwestern Ontario, Canada: new constraints from U–Pb geochronology at the Goldcorp High-grade Zone, Red Lake mine and at the Madsen mine. Econ Geol 99:1611–1641

Dubessy J, Boiron M-C, Moissette A, Monnion C, Sretenskaya N (1992) Determination of water, hydrates and pH in fluid inclusions by micro-Raman spectrometry. Eur J Mineral 4:885–894

Fyfe W, Price NJ, Thompson AB (1978) Fluids in the earth's crust. Developments in Geochemistry 1. Elsevier, New York, p 383

Fyon JA, Troop DG, Marmont S, Macdonald AJ (1989) Introduction of gold into Archean crust, Superior Province, Ontario—coupling between mantle-initiated magmatism and lower crustal thermal maturation. Econ Geol Monogr 6:479–490

Gammons CH, Williams-Jones AE (1997) Chemical mobility of gold in the porphyry-epithermal environment. Econ Geol 92:45–59

Garba I, Akande SO (1992) The origin and significance of non-aqueous $CO_2$ fluid inclusions in the auriferous veins of Bin Yauri, northwestern Nigeria. Mineral Depos 27:249–255

Goldstein RH, Reynolds TJ (1994) Systematics of fluid inclusions in diagenetic minerals. SEPM Short Cour 31:1–199

Groves DI, Goldfarb RJ, Robert F, Hart CJR (2003) Gold deposits in metamorphic belts: overview of current understanding, outstanding problems, future research, and exploration significance. Econ Geol 98:1–29

Guha J, Lu H-Z, Dubé B, Robert F, Gagnon M (1991) Fluid characteristics of vein and altered wall rock in Archean Mesothermal gold deposits. Econ Geol 86:667–684

Heinrich CA, Günther D, Audédat A, Ulrich T, Frischknecht R (1999) Metal fractionation between magmatic brine and vapor, determined by microanalysis of fluid inclusions. Geology 27:755–758

Hollister LS (1988) On the origin of $CO_2$-rich inclusions in migmatites. J Metamorph Geol 6:467–474

Hollister LS (1990) Enrichment of $CO_2$ in fluid inclusions in quartz by removal of $H_2O$ during crystal-plastic deformation. J Struct Geol 12:895–901

Johnson EL, Hollister LS (1995) Syndeformational fluid trapping in quartz: determining the pressure–temperature conditions of deformation from fluid inclusions and the formation of pure $CO_2$ fluid inclusions during grain boundary migration. J of Metamorph Geol 13:239–249

Klemd R (1998) Comment on the paper by Schmidt Mumm et al. High $CO_2$ content of fluid inclusions in gold mineralizations in the Ashanti Belt, Ghana: a new category of ore forming fluids? (Mineral Depos 32:107–118, 1997). Mineral Depos 33:317–319

Lowenstein JB (2001) Carbon dioxide in magmas and implications for hydrothermal systems. Mineral Depos 36:490–502

MacGeehan PJ, Hodgson CJ (1982) Environments of gold mineralization in the Campbell, Red lake and Dickenson mines, Red Lake district, Ontario. In: Geology of Canadian gold deposits. Canadian Institute of Mining and Metallurgy, Special Volume 24:184–207

MacGeehan PJ, Sanders T, Hodgson CJ (1982) Meter-wide veins and a kilometer-wide anomaly: wall-rock alteration at the Campbell Red Lake and Dickenson gold mines, Red Lake District, Ontario. Can Mining Metall Bull 75:90–102

Mathieson NA, Hodgson CJ (1984) Alteration, mineralization, and metamorphism in the area of East South "C" ore zone, 24th level of the Dickenson mine, Red Lake, northwestern Ontario. Can J Earth Sci 21:35–52

Mikucki EJ (1998) Hydrothermal transport and depositional processes in Archean lode-gold systems: a review. Ore Geol Rev 13:307–321

Naden J, Shepherd TJ (1989) Role of methane and carbon dioxide in gold deposition. Nature 342:793–795

Newton RC, Manning CE (2000) Quartz solubility in $H_2O$–NaCl and $H_2O$–$CO_2$ solutions at deep crust-upper mantle pressures and temperatures: 2–15 kbar and 500–900°C. Geochim Cosmochim Acta 64:2993–3005

Newton RC, Smith JV, Windley BF (1980) Carbonic metamorphism, granulites and crustal growth. Nature 288:45–50

Parker JR (2000) Gold mineralization and wall rock alteration in the Red Lake greenstone belt: a regional perspective. Summary of Field Work and Other Activities, Ontario Geological Survey, Open File Report 6032, p.22–1 to 22–28

Penczak R, Mason R (1999) Characteristics and origin of Archean premetamorphic hydrothermal alteration at the Campbell gold mine, northwestern Ontario, Canada. Econ Geol 94:507–528

Penczak R, Mason R (1997) Metamorphosed Archean epithermal Au–As–Sb–Zn–(Hg) vein mineralization at the Campbell Mine, Northwestern Ontario. Econ Geol 92:696–719

Poulsen KH, Robert F, Dubé B (2000) Geological classification of Canadian gold deposits. Geol Surv Can Bull 540:1–106

Ridley JR, Diamond LW (2000) Fluid chemistry of orogenic lode gold deposits and implications for genetic models. In: Hagemann SG, Brown PE (eds) Gold in 2000. Rev Econ Geol 13:146–162

Robert F, Kelly WC (1987) Ore-forming fluids in Archean gold-bearing quartz veins at Sigma mine, Abitibi greenstone belt, Quebec, Canada. Econ Geol 82:1464–1482

Rogers JA (1992) The Arthur W. White mine, Red Lake area, Ontario: detailed structural interpretation - the key to successful grade control and exploration. Can Mining Metall Bull 85:37–44

Salvi S, Williams-Jones AE (2003) bulk analysis of volatiles in fluid inclusions. In: Samson I, Anderson A, Marshall D (eds) Fluid inclusions: analysis and interpretation. Mineralogical Association of Canada, Short Course Series 32:247–278

Sanborn-Barrie M, Skulski T, Parker J (2001) Three hundred millions of years of tectonic history recorded by the Red Lake greenstone belt, Ontario. Geological Survey of Canada, Current Research 2001-C19

Sanborn-Barrie M, Skulski T, Parker JR (2004) Geology, Red Lake greenstone belt, western Superior Province, Ontario. Gelogical Survey of Canada, Open File 4594. 1:50 000 scale color map

Santosh M (1986) Carbonic metamorphism of charnockites in the southwestern Indian Shield: a fluid inclusion study. Lithos 19:1–10

Santosh M, Tanaka K, Yoshimura Y (2005) Carbonic fluid inclusions in ultrahigh-temperature granitoids from southern India. C.R. Geosci 337:327–335

Sarkar S, Santosh M, Dasgupta S, Fukuoka M (2003) Very high density $CO_2$ associated with ultrahigh-temperature metamorphism in the Eastern Ghats granulite belt, India. Geology 31:51–54

Schmidt Mumm A, Oberthür T, Vetter U, Blenkinsop TG (1997) High $CO_2$ content of fluid inclusions in gold mineralizations in the Ashanti Belt, Ghana: a new category of ore forming fluids? Mineral Depos 32:107–118

Schmidt Mumm A, Oberthür T, Vetter U, Blenkinsop TG (1998) High $CO_2$ content of fluid inclusions in gold mineralizations in the Ashanti Belt, Ghana: a new category of ore forming fluids?—a reply. Mineral Depos 33:320–322

Stuart FM, Ellam RM, Harrop PJ, Fitton JG, Bell BR (2000) Constraints on mantle plumes from the helium isotopic composition of basalts from the British Tertiary Igneous Province. Earth Planet Sci Lett 177:273–285

Tarnocai C (2000) Archean gold mineralization at the Campbell mine, eastern Red Lake greenstone belt, western Superior Province of Canada. Ph.D. thesis, University of Ottawa, 227p

Thompson PH (2003) Toward a new metamorphic framework for gold exploration in the Red Lake greenstone belt. Ontario Geological Survey Open File report 6122, 51 p

Touret JLR (2001) Fluids in metamorphic rocks. Lithos 55:1–25

Twomey T, McGibbon S (2001) The geological setting and estimation of gold grade of the High-grade Zone, Red Lake Mine, Goldcorp Inc. Explor Mining Geol 10:19–34

Van den Kerkhof A, Thiéry R (2001) Carbonic inclusions. Lithos 55:49–68

Walther JV, Orville PM (1983) The extraction-quench technique for determination of the thermodynamic properties of solute complexes: application to quartz solubility in fluid mixtures. Am Mineral 68:731–741

Watson EB, Brenan JM (1987) Fluids in the lithosphere, 1. Experimentally-determined wetting characteristics of $CO_2$–$H_2O$ fluids and their implications for fluid transport, host-rock physical properties, and fluid inclusion formation. Earth Planet Sci Lett 85:497–515

Wille SE, Klemd R (2004) Fluid inclusion studies of the Abawso gold prospect, near the Ashanti Belt, Ghana. Mineral Depos 39:31–45

Williams-Jones AE, Heinrich CA, Migdisov AA (2005) Vapor as a medium for the transport of metals: implications for ore deposit modeling. Geochim Cosmochim Acta 69:A733

Xavier RP, Foster RP (1999) Fluid evolution and chemical controls in the Fazenda Maria Preta (FMP) gold deposit, Rio Itapicuru Greenstone Belt, Bahia, Brazil. Chem Geol 154:133–154

Zakaznova-Iakovleva VP, Migdisov AA, Suleimenov OM, Williams-Jones AE, Alekhin YuV (2001) An experimental study of stibnite solubility in gaseous hydrogen sulphide from 200 to 320 degrees C. Geochim Cosmochim Acta 65:289–298